From species sorting to mass effects: spatial network structure mediates the shift between metacommunity archetypes

ECOGRAPHY

Research

From species sorting to mass effects: spatial network structure mediates the shift between metacommunity archetypes

Yuka Suzuki and Evan P. Economo

Y. Suzuki (https://orcid.org/0000-0003-0930-5591) ✉ (yuka.suzuki@oist.jp) and E. P. Economo (https://orcid.org/0000-0001-7402-0432), Biodiversity and Biocomplexity Unit, Okinawa Inst. of Science and Technology Graduate Univ., Okinawa, Japan.

Ecography
44: 1–12, 2021
doi: 10.1111/ecog.05453

Subject Editor:
Christine N. Meynard
Editor-in-Chief:
Jens-Christian Svenning
Accepted 23 December 2020

Local assemblages are embedded in networks of communities connected by dispersal, and understanding the processes that mediate this local–regional interaction is central to understanding biodiversity patterns. In this network (i.e. metacommunity), the strength of dispersal relative to the intensity of environmental selection typically determines whether local communities are comprised of species well-adapted to the local environment (i.e. species sorting) or are dominated by regionally successful species that may not be locally adapted (i.e. mass effects), which by extension determines the capacity of the landscape to sustain diversity. Despite the fundamentally spatial nature of these dispersal-mediated processes, much of our theoretical understanding comes from spatially implicit systems, a special case of spatial structure in which patches are all connected to each other equally. In many real systems, both the connections among patches (i.e. network topology) and the distributions of environments across patches (i.e. spatial autocorrelation) are not arranged uniformly. Here, we use a metacommunity model to investigate how spatial heterogeneities may change the balance between species sorting versus mass effects and diversity outcomes. Our simulations show that, in general, the spatially implicit model generates an outlier in biodiversity patterns compared to other networks, and most likely amplifies mass effects relative to species sorting. Network topology has a strong effect on metacommunity outcome, with topologies of sparse connections and few loops promoting sorting of species into suitable patches. Spatial autocorrelation is another key factor; by interacting with spatial topology, intermediate-scale clusters of similar patches can emerge, leading to a reduction of regional competition, and hence maintenance of gamma diversity. These results provide a better understanding of the role that complex spatial landscape structure plays in metacommunity processes, a necessary step to understanding how metacommunity processes relate to biodiversity conservation.

Keywords: biodiversity, landscape ecology, metacommunity assembly, spatial scale, source–sink effects

NORDIC SOCIETY OIKOS

www.ecography.org

Introduction

Understanding the processes underlying biodiversity patterns across local and regional scales is one of the central challenges in ecology. In recent decades, the role of spatial heterogeneity in the environment interacting with dispersal processes has been increasingly recognized as critical to ecological outcomes (Crowley 1981, Chesson 2000, Chase and Leibold 2002, Amarasekare 2003, Witman et al. 2004, Cottenie 2005, Randin et al. 2006, Kadmon and Allouche 2007, Harrison and Cornell 2008, Myers and Harms 2009, Heino 2011). These research themes have been unified under the metacommunity ecology framework (Kneitel and Chase 2004, Leibold et al. 2004, Vellend 2016), expanding the scope of local-scale community ecology to landscapes and regions. Leibold et al. (2004) delineated four major archetypes in metacommunity ecology that represent different classes of ecological dynamics: patch dynamics, neutral dynamics, species sorting and mass effects. These dynamics emerge from the interplay of more fundamental processes (sensu Vellend 2016), i.e. dispersal, drift, selection and speciation, which in turn reflect the interaction of biological aspects with the physical environment of the landscape. Understanding how the relative strengths of these processes contribute to higher level dynamics remains an essential goal of the field (Leibold and Loeuille 2015, Thompson et al. 2020).

A key early result in metacommunity ecology relates to the transition between 'species-sorting' and 'mass-effect' archetypes as dispersal increases (Mouquet and Loreau 2002, 2003, Loreau et al. 2003, Cadotte 2006, Shanafelt et al. 2015, Thompson and Gonzalez 2016, Leibold et al. 2017). Under species sorting, species generally exist in patches where they are highly adapted and few places where they are suboptimal. This leads to relatively high beta diversity and low alpha diversity, as the landscape becomes a mosaic of locally well adapted species. At very high dispersal, regional competition is too strong for local selection to overcome inputs from dispersal, leading to 'mass effects'. As species that tend to be better competitors across the entire landscape become abundant, the metacommunity becomes both more homogenized and more depauperated. The transition between species-sorting (local selection only) and mass-effect (dispersal dominant) regimes can occur as a consequence of two processes related to dispersal: source–sink effects and regional competition. The source–sink effect, a process in which dispersal from an adjacent source to sink populations leads to an increased opportunities for local coexistence (higher alpha diversity) (Amarasekare and Nisbet 2001), allows for stable mal-adaptations (Dias 1996). Alternatively, regional competition can be the dominant process and reduce regional diversity by allowing only the most fit species (with fitness averaged across heterogeneity in the landscape) to persist in the metacommunity, while many locally superior but regionally inferior species are excluded. (Mouquet and Loreau 2002) (Fig. 1).

While dispersal is clearly a key mediator of the transition from species-sorting to mass-effect dynamics, we have much to learn about other factors that may affect this transition. Moreover, there may be factors that prevent the realization of certain metacommunity states, such as local coexistence. The Mouquet and Loreau model (M&L model hereafter) is an eminently rational starting point for investigating metacommunity dynamics containing a number of simplifications. The constraints set for the simplifications need further exploration to evaluate the generality of the results. Previous work, for example, has extended the M&L model by exploring the effects of species-level variation in dispersal rate (Loreau et al. 2003), time-varying environments (Shanafelt et al. 2015) and the impact of harvest by humans (Shanafelt et al. 2018).

One key limitation of the M&L model is the spatially implicit assumption. Metacommunity models are inherently spatial, in the relationship between local and regional dynamics, with dispersal rates linking local dynamics

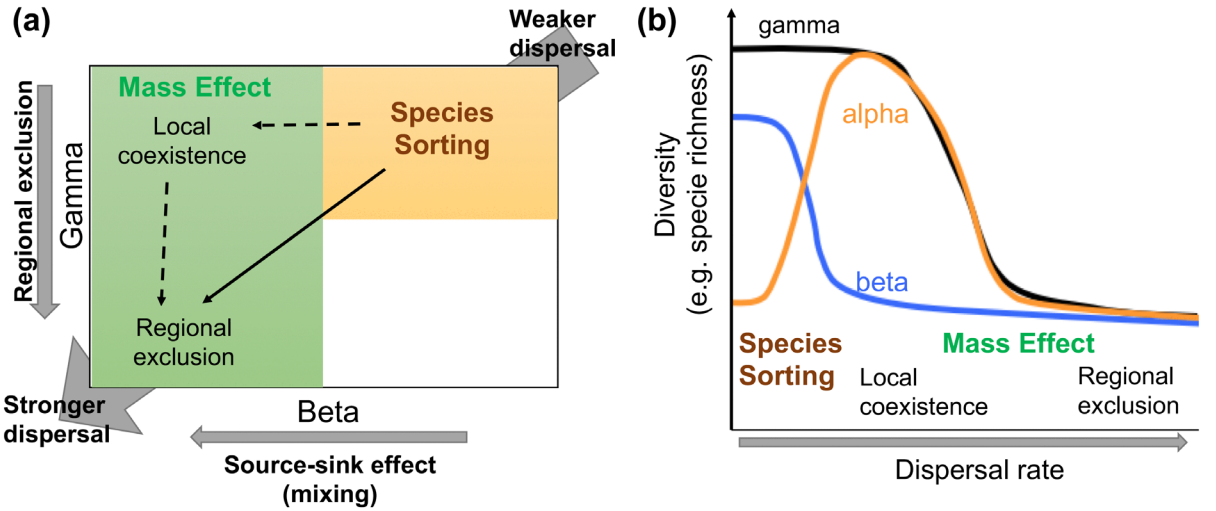

Figure 1. Overview of the metacommunity framework in this study. (a) Relationship between species-sorting and mass-effect archetypes and metacommunity processes. (b) Biodiversity patterns suggested by the M&L model. This biodiversity patterns predicted by the M&L model corresponds to the trajectory shown with dashed arrows in panel (a).

(Tilman 1994). However, many of the foundational theoretical results are based on a spatially implicit metacommunity structure (Mouquet and Loreau 2003, Loreau et al. 2003, Shanafelt et al. 2015). Studies using the M&L model with spatially implicit assumption predict that local diversity can increase at an intermediate dispersal rate and decreases after the threshold, when regional competition becomes significant. In other words, there are three phases in the diversity–dispersal curve: a) low alpha diversity with local selection dominant at small dispersal rate, b) higher alpha diversity (local coexistence, with stable mal-adaptations) with both local selection and source–sink effect dominant at a larger dispersal rate smaller than the threshold and c) lower alpha diversity due to regional competitive exclusion at a dispersal rate larger than the threshold (Fig. 1). Altogether, these generate a hump-shaped relationship between the local diversity and dispersal rate with a peak at the intermediate dispersal rate, indicating local coexistence of locally optimal and maladapted species. Here, communities are separated from each other, but in a homogeneous way that does not reflect variation in inter-patch distances or allow for non-random patterns in how environments are distributed across the landscape. In contrast, real systems have patches that are connected in complex ways, reflecting the physiographic structure of the world and the movement of organisms across landscapes (Legendre and Fortin 1989, Wiens 1989, Leibold and Norberg 2004, Hillebrand and Matthiessen 2009, Heino et al. 2015).

Several previous studies highlighted the significance of complex spatial structures in metacommunity dynamics. Among theoretical studies, Economo and Keitt (2008) suggested that explicit spatial structure can yield higher gamma diversity compared to a well-mixed metacommunity of the same size. Muneepeerakul et al. (2007) and Morrissey and de Kerckhove (2009) also found that dendritic systems compared to linear or two-dimensional lattice landscapes support higher genetic diversity. Thompson et al. (2017) showed that dispersal rate influences the relative contribution of species sorting and mass effects to spatial insurance, while focusing on overall dispersal rate as the main parameter in metacommunity dynamics. In a large and complex spatial structure, environmental heterogeneity can be measured by spatial autocorrelation in environment, which is another parameter that affects population dynamics (Petchey et al. 1997). In addition to such theoretical studies, Chisholm et al. (2011) empirically showed that spatial structure alters biodiversity levels in metacommunity, which becomes more evident when environmental heterogeneity is present. These studies highlight that complex spatial structure in nature, including the structure of dispersal and spatial autocorrelation, can play a key role in governing metacommunity assembly. They also demonstrate that network approaches are powerful ways to represent complex spatial structures and explore these structure's effects. Moreover spatial ecological networks have important relevance for biodiversity conservation (Gonzalez et al. 2017).

Despite these advances which point toward the importance of spatially explicit processes in metacommunity dynamics, we have no clear understanding of how complex spatial structure mediates transitions between metacommunity archetypes. Here, we extend the M&L model to accommodate two aspects of complex spatial structure: variation in network topology, and spatial autocorrelation in the environment. We ask, when considering the balance between species sorting and mass effects a) whether the lessons of the spatially implicit model hold when considering more complex spatially explicit environments, and specifically b) what the roles of network topology and spatial autocorrelation are in the transition between species sorting and mass effects. We address these questions using a simulation approach to probe the dependence of spatial organization of biodiversity (alpha, beta, gamma) on dispersal rates and on different spatially explicit models.

Methods

Model construction

The model we use is based on the one suggested by Mouquet and Loreau (2002, 2003), which is a lottery model (Chesson 1985, Muko and Iwasa 2000) with discrete time steps. It focuses upon the characteristics of certain sessile or sedentary marine organisms such as corals that mass spawn (synchronized spawning) and disperse passively. This model also assumes that local communities have infinite carrying capacity, and the main response variable is the relative abundance of species, not the absolute population size. This removes the influence of finite size effects such as demographic stochasticity, and thus the model has deterministic dynamics. These assumptions (from the original M&L model) allow us to highlight the effects of dispersal on species sorting and mass effects while excluding confounding factors such as the behavioral complexities of active dispersal and stochastic finite-size effects. We extend their model to metacommunity systems with explicit spatial structure in addition to a complete network, which corresponds to a spatially implicit model. We assume that the settlement success of each species is perfectly proportional to the species abundance based on individuals in the pre-settlement phase after dispersal. However, this model could be easily modified into a stochastic model by introducing multinomial sampling. The metacommunity model is coded in Julia (Bezanson et al. 2017).

We use a metacommunity of $N=100$ patches with unique environmental conditions and $S=20$ species. Let a_{lk} be the dispersal rate from community l to k. The network structure of the metacommunity enters the model through the matrix of all a_{lk} describing the dispersal of individuals across the metacommunity. We assume that after the reproduction process within each community, the fraction $1-\sum_{k,k\neq l}^{N} a_{lk}$ of individuals in community l stay in the community, and a_{lk} disperse from community l to community k.

The simulated processes were reproduction in each local community, dispersal between local communities,

immigration from the regional species pool to local patches, and settlement. Note that dispersal and settlement processes are distinguished, such that dispersers first arrive at a local patch and then all or some of them settle. We refer to individuals in the pre-settlement stage as the 'local pool' of its local community. Let $P_{ik}(t)$ be the fraction of sites occupied by species i in community k at time t, and $q_{ik}(t)$ as the number of individuals of species i in the local pool of local community k. Through the reproduction process, the fraction of species i in local community l becomes $P_{it}c_{il}$, where c_{il} is the reproduction rate of species i in community l, which hence reflects its fitness. Then the fraction $\left(1-\sum_{j=1,j\neq k}^{N}a_{kj}\right)$ of all the individuals in a community stay, and $\sum_{j=1,j\neq k}^{N}a_{kj}$ leave for the regional pool. These processes can be written as follows:

$$\text{reproduction}: \quad q_{ik}(t) = c_{ik}P_{ik}(t) \tag{1}$$

$$\text{dispersal}: \quad q'_{ik}(t) = \sum_{l=1,l\neq k}^{N}\left(a_{lk}q_{il}(t)\right) + \left(1-\sum_{j=1,j\neq k}^{N}a_{kj}\right)q_{ik}(t) \tag{2}$$

$$\text{immigration}: \quad Pr\left\{q'_{ik}+1 \,|\, q'_{ik}\right\} = \nu P_i^{\text{reg}} \tag{3}$$

ν is the immigration rate from the regional pool to each community, and P_i^{reg} denotes the relative species abundance in the regional pool. We assume that all individuals are replaced by offspring every generation. Therefore, the number of individuals of species i in community k after dispersal becomes

$$q'_{ik}(t) = \sum_{l=1,l\neq k}^{N}a_{lk}c_{il}P_{il}(t) + \left(1-\sum_{j=1;j\neq k}^{N}a_{kj}\right)c_{ik}P_{ik}(t) \tag{4}$$

The matrix notation of this equation is

$$\mathbf{q'(t)} = (\mathbf{C}\circ\mathbf{P})\mathbf{A} + \mathbf{Z}\circ\mathbf{C}\circ\mathbf{P} \tag{5}$$

where $\mathbf{Z}$ is a S-by-N matrix, $\mathbf{Z}=\mathbf{I}-\mathbf{U}$, $\mathbf{U}$ is a S-by-N matrix, $u_{ik}=1-\sum_{j=1}^{N}a_{kj}$, and $a_{kk}=0$. $\mathbf{I}$ is a S-by-N matrix, with elements all equal to 1. $\circ$ denotes the Hadamard product.

Assuming the lottery system for competition over space (i.e. random allocation of unoccupied sites to pre-settlement individuals) the probability that an individual of species i is randomly chosen and occupies an unoccupied site in community k (r_{ik}) becomes proportional to $q'_{ik}(t)$:

$$r_{ik} = q'_{ik} \,/\, \sum_{i=1}^{S}q'_{ik} \tag{6}$$

The right-hand side can be written in matrix notation as

$$\mathbf{q'} \oslash (\mathbf{Iq'}) \tag{7}$$

where $\oslash$ is the Hadamard division.

With the immigration process described in Eq. 3,

$$r_{ik} = (1-\nu)q'_{ik} \,/\, \sum_{i=1}^{S}q'_{ik} + \nu P_i^{\text{reg}} \tag{8}$$

The right-hand side can be written in matrix notation as

$$(1-\nu)\mathbf{q'} \oslash (\mathbf{Iq'}) + \nu\mathbf{1}\mathbf{P}^{\text{reg}\,\mathrm{T}} \tag{9}$$

where $\mathbf{1}$ is a S-by-1 column vector of ones, and $\mathbf{P}^{\text{reg}}$ is a S-by-1 column vector whose i-th element is P_i^{reg}.

The frequency P_{ik} in this deterministic model in generation $t+1$ will then become

$$\mathbf{P}_{t+1} = (1-\nu)\mathbf{q'}_t \oslash (\mathbf{Iq'}_t) + \nu\mathbf{1}\mathbf{P}^{\text{reg}\,\mathrm{T}} \tag{10}$$

We chose to evaluate a closed metacommunity ($\nu=0$) for our experiments as immigration from the outside simply raised the minimum diversity levels without changing the overall patterns and conclusions.

Stationary condition

We ran each simulation until the community dynamics reached a stationary state that satisfied the following condition:

$$\sum_{i,k}P_{ik,t} \leq \text{tolerance} \tag{11}$$

where tolerance was $0.0000001 \times S \times N$ ($S=20$: the total number of species, $N=100$: the number of local communities).

Reproduction rate

Species' traits are characterized by $x_i \in [0,1]$. E_l denotes the environmental condition in community l ($E_l \in [0,1]$). x_i and E_l are unique to species and patches, respectively. The potential reproduction rate c_{il} is defined as

$$c_{il} = \frac{1}{\sqrt{2h\pi}}\exp-\frac{(E_l-x_i)^2}{2h} \tag{12}$$

This indicates that the species with x_i closer to E_l in community l is more successful in the competition. h corresponds to the variance in a Gaussian distribution, so a larger h corresponds to weaker local selection. This model assumes that the difference in reproduction rate between species is the only interspecific difference that directly makes the chance of settlement different among species.

Diversity measure

We calculate alpha (local), beta (between-patch) and gamma (regional) diversity based on the outputs of metacommunity simulations on five different spatial topologies at different levels of spatial autocorrelation and different strengths of local selection. These diversity indices were calculated based on the multiplicative partition of the effective number of species (Hill 1973) with the Gini–Simpson index (Jost 2006, 2007, Jost et al. 2010) (Fig. 4) as well as species richness (Fig. 5). The Gini–Simpson index is $1 - \lambda$, where λ is the Simpson concentration, which is defined as

$$\lambda = \sum_{i=1}^{S} p_{ij}^2$$

This is also known as the probability of identity. Note that p_{ij} is the relative species abundance of species i in community j, that is, the proportion of occupied sites by species i in community k, where Q_{ik} is the number of individuals of species i in community k:

$$p_{ik} = Q_{ik} / \sum_{i}^{S} Q_{ik}$$

Jost (2006) showed that the gamma and alpha components of the Simpson concentration can be written as

$$\lambda_\gamma = \sum_{i=1}^{S} \left(\sum_{j=1}^{N} w_j p_{ij} \right)^2 \tag{13}$$

$$\text{and} \quad \lambda_\alpha = \sum_{j=1}^{N} \left(w_j^2 \sum_{i=1}^{S} p_{ij}^2 \right) / \sum_{j=1}^{N} w_j^2 \tag{14}$$

The multiplicative partition in terms of the Simpson concentration becomes

$$\lambda_\beta = \lambda_\gamma / \lambda_\alpha \tag{15}$$

We set $w_j = w$ for all j, so that the diversity measure satisfies the condition for strict concavity, i.e. average local (alpha) diversity does not exceed global (gamma) diversity. For the beta diversity to have a monotonic relation with the degree of differentiation between N communities, the weights should be equal to $1/N$.

Taking the inverse of each component of the Simpson concentration, $1/\lambda_\gamma$, $1/\lambda_\alpha$ and $1/\lambda_\beta$ become gamma, alpha and beta diversity, respectively.

Network construction

We use five different network topologies: Watts–Strogatz ('small-world') (Watts and Strogatz 1998), grid, linear, tree and complete networks (Fig. 3). Kininmonth et al. (2010) investigated the larval connectivity model of reef fish estimated by James et al. (2002) and showed that the network resembled a small-world network with hub structure. The linear topology is a network structure with 100 nodes arranged on a line, the grid topology is a 10×10 grid, and complete network is a network in which each node is connected to all other nodes, which corresponds to the spatially implicit network often used in previous studies (Mouquet and Loreau 2002, 2003). We generated these five types of networks with 100 nodes and edges whose weights are equal in a topology and defined such that the total dispersal rate becomes the same on all five different topologies. We used the grid topology to observe the effect of having alternative paths to get one community to another, in comparison with linear network. We used NetworkX in Python3 (Hagberg et al. 2008), to generate a small-world network and a tree network. For the small-world network, we used the function connected_watts_strogatz_graph ($n = 100$, $k = 4$, $p = 0.1$; n: the number of nodes, k: each node is joined with its k nearest neighbors in a ring topology, p: the probability of rewiring each edge). For the tree topology, we first generated a rooted tree with the function balanced_tree ($r = 3$, $h = 4$), and randomly removed leaf nodes (nodes with a single neighbor), so that the total number of nodes in the tree network becomes 100. The matrix **A** in Eq. 5, where a_{lk} represents the dispersal rate from community l to k, reflects network topology. We used total dispersal rates 0.0005, 0.005, and from 0.05 to 0.4 with interval 0.05. Here, the total dispersal rate is the fraction of the entire metacommunity that disperses in each generation. Since the networks vary in the number of total links, the dispersal strengths of each link were adjusted (by downweighting links in networks with more connections) to equalize the number of total dispersers and provide a fair comparison among topologies.

Environmental conditions and spatial autocorrelation

As defined in Eq. 12, the environmental condition E_k affects the reproduction rate of species i in community k, c_{ik}. We define the species trait value as $x_{i+1} = x_i + 1/S$, $(x_1 = 0)$ for $i = 1, \ldots, S - 1$. Environmental condition, E_k also takes a value between 0.0 and 1.0; $E_k = E_{k-1} + 1/N$, $E_1 = 0$ for local community k.

To assign each E_k value to a specific local community k, we first optimized spatial arrangement of environmental conditions using spatial autocorrelation as the target of optimization. We conducted this optimization on all networks

except the complete network because there is only a single level of spatial autocorrelation that a complete network can take. We defined the spatial autocorrelation of a network as the inverse of ρ, the sum of the difference in environmental conditions between every connected pair of patches, as denoted below:

$$\rho = \sum_{k,l}^{N} |E_k - E_l| \times a_{kl} \quad (16)$$

where $a_{kl} = 1$ if patch k and l are connected and $a_{kl} = 0$ otherwise. For a complete network, $\rho = 1666.5$ regardless of the spatial arrangement of environmental conditions. The optimization algorithm is as follows: 1) randomly assign E_k to each patch and calculate ρ; 2) randomly choose two pairs of patches (patch i and j, k and l); 3) see if swapping the environmental conditions between both pairs (i and j, k and l) decreases ρ; 4) if ρ decreases (and hence increases spatial autocorrelation), update the environmental condition by adopting the arrangement after the swapping; 5) repeat 1–4 for 11 000 times. We ran this algorithm five times on each network topology and observed ρ asymptotically decreased (Fig. 2).

Based on this result, we chose three arrangements of environmental conditions for each topology: a random arrangement (lowest spatial autocorrelation), the arrangement chosen by the above optimization (highest spatial autocorrelation), and the first arrangement in the optimization that had $\rho < 20$ (intermediate spatial autocorrelation). Note that the value ρ for the lowest and highest spatial autocorrelation depends on the topology (Fig. 3).

Results

We observed the previously known (Mouquet and Loreau 2002, 2003) hump-shaped relationship between alpha diversity and dispersal rate for the complete network when $h = 0.1$ (Fig. 4, 5, second rows), but this relationship was hardly observed on other topologies and alpha diversity remained small across different dispersal rates. For smaller h, there was a pronounced difference in alpha diversity for the complete network when calculated using Gini–Simpson (Fig. 4) and richness-based (Fig. 5) diversity measures. In contrast, we observed the general trend of declining gamma diversity with increasing dispersal rate on all topologies. We also found slower and more gradual declines in beta diversity with increasing dispersal on the four networks compared to the complete network.

We investigated how spatial topology affected the balance between local and regional competitions by manipulating the parameter h (the smaller h, the stronger local selection) and spatial autocorrelation of environmental conditions. Gamma diversity decreased as h increased (first columns in Fig. 4). When local selection was weak (especially when $h = 10$), gamma, alpha and beta diversities all became close to 1 as dispersal increased. In other words, all the local patches, or the entire metacommuntiy, retained few species and became homogenized except for the high spatial autocorrelation case simulated using the linear and tree networks. Under weaker local selection (third and fourth rows in Fig. 4), gamma and beta diversity on non-complete networks, especially for linear and tree topologies, became higher with increased environmental autocorrelation.

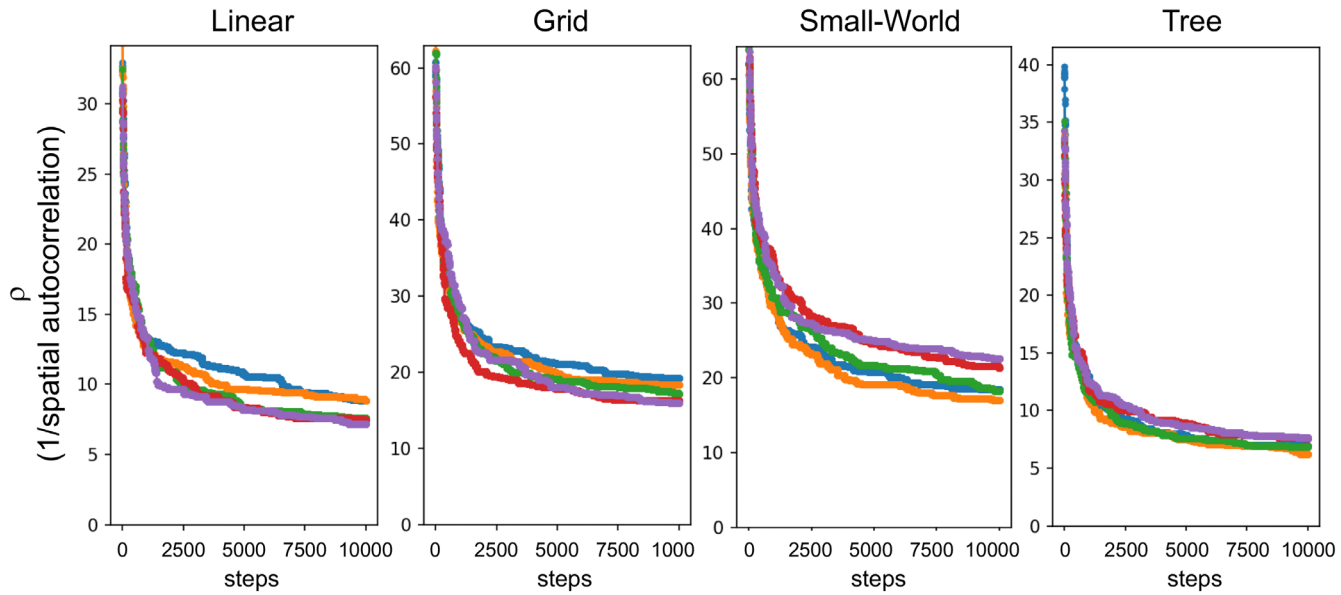

Figure 2. Changes in ρ (1/spatial autocorrelation) during the optimization process.

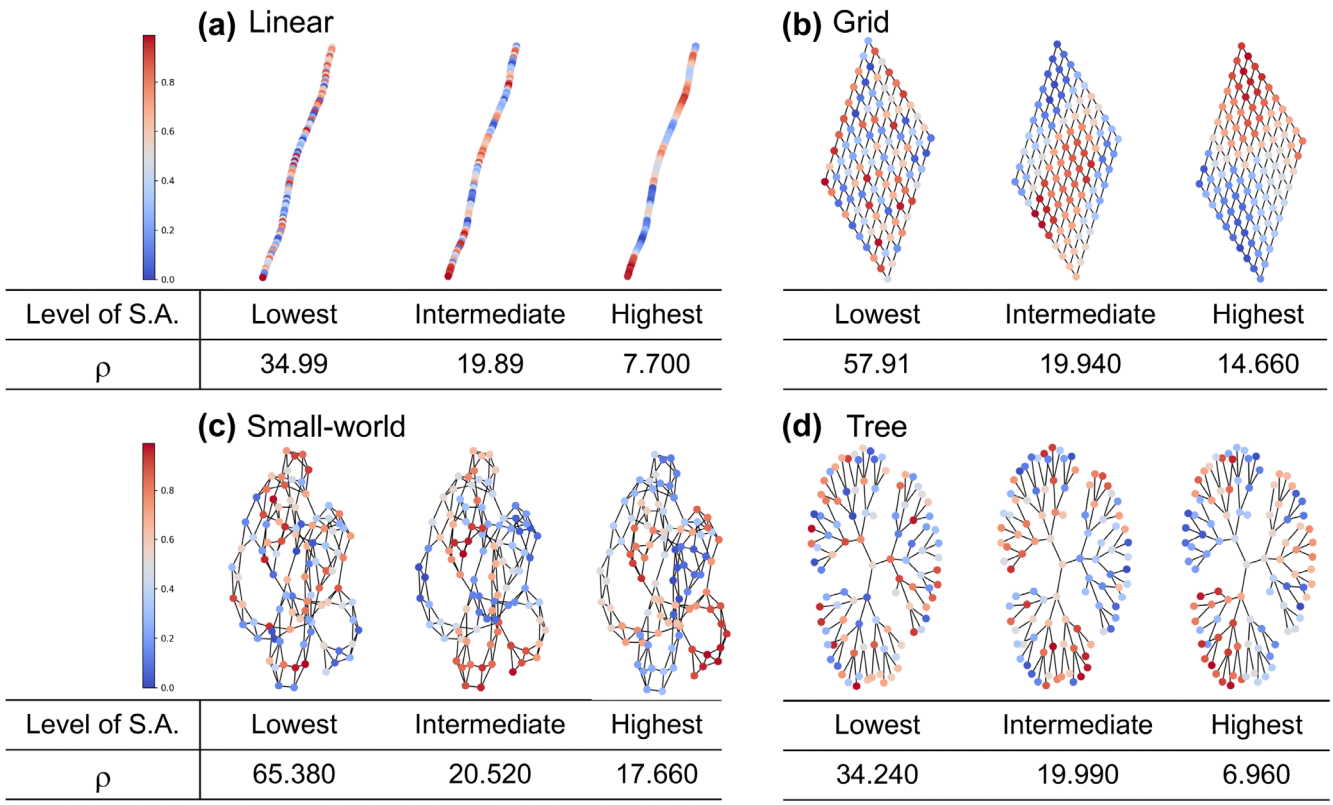

Level of S.A.	Lowest	Intermediate	Highest
ρ	34.99	19.89	7.700

Lowest	Intermediate	Highest
57.91	19.940	14.660

Level of S.A.	Lowest	Intermediate	Highest
ρ	65.380	20.520	17.660

Lowest	Intermediate	Highest
34.240	19.990	6.960

Figure 3. Network topologies and spatial arrangements of environmental conditions with three different levels of spatial autocorrelation (S.A.). (a) Linear, (b) grid, (c) small-world, (d) tree networks. In the complete topology each node is connected to all the other nodes. Thus, the complete network can take only one level of spatial autocorrelation, ρ = 1666.5.

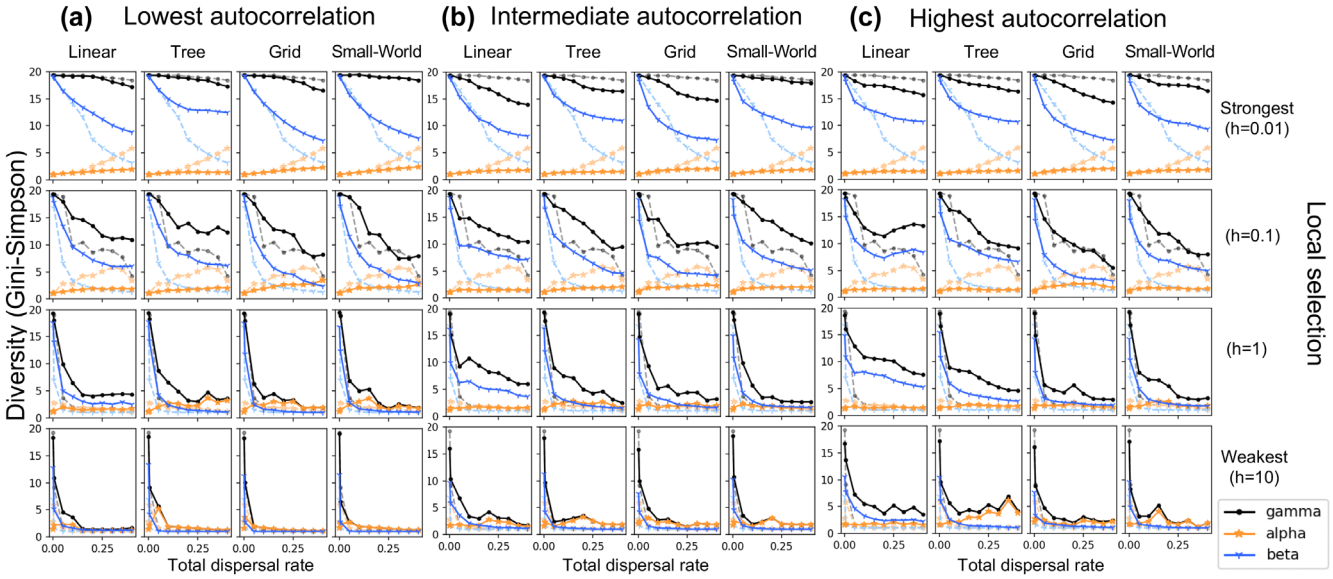

Figure 4. Diversity measures across different *h* values and three different levels of spatial autocorrelation simulated using linear, grid, small-world and tree networks. We observed topology-dependence of alpha, beta, gamma diversity. Note that diversity measured on the complete network (dashed lines in lighter colors) is more so extreme than general. Networks that consist of line-shaped components, such as linear and tree, tended to generate high beta diversity. Note that the spatial autocorrelation level on complete network is a fixed value. Diversity values were calculated based on the Gini–Simpson index, and we used multiplicative beta diversity (Jost 2006, Jost et al. 2010). See Figure 6 for an alternative view to associate biodiversity patterns with mass effects and species sorting.

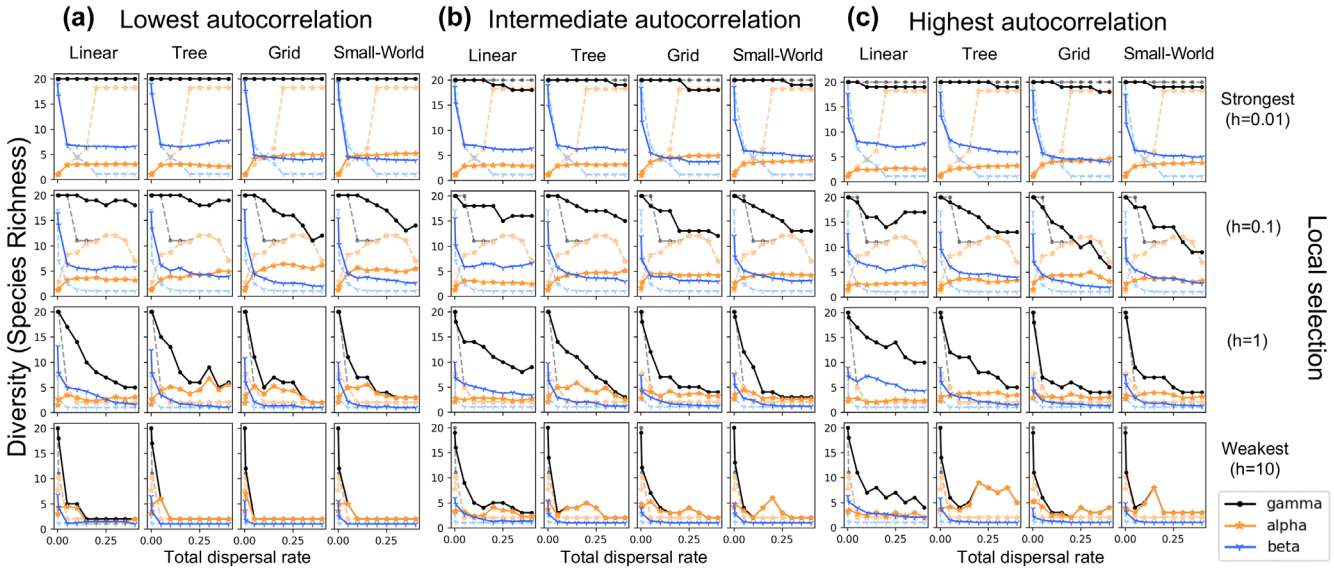

Figure 5. Species richness-based diversity measures across different h values among the three different levels of spatial autocorrelation simulated using linear, grid, small-world and tree networks. We observed topology-dependence of alpha, beta, gamma diversity. We calculated diversity values based on species richness and used multiplicative beta diversity with equal weights on all local communities (Jost et al. 2010). We excluded the fraction of species i in local community k to calculate diversity when $P_{ik} < 0.01$ to compare with the results from Mouquet and Loreau (2003). See Figure 6 for an alternative view in associating biodiversity patterns with mass effects and species sorting.

Figure 6 provides an alternative view of the biodiversity patterns generated through simulations, in a manner corresponding to Fig. 1. The trajectory followed by metacommunities with the complete network followed is clearly different from other spatial topologies.

Discussion

Our analysis of how dispersal controls metacommunity dynamics in spatially complex environments adds important corollaries to some central results in metacommunity

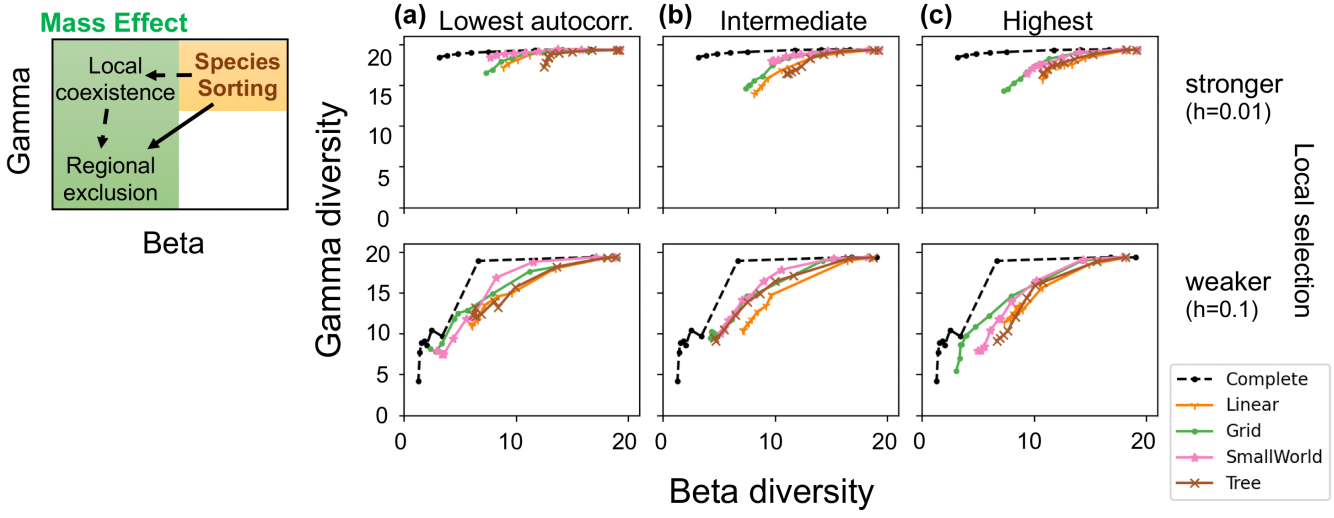

Figure 6. Beta–gamma diversity plot of simulation results on the five spatial structures for dispersal rates ranging between 0.4 (top right) and 0.0005 (bottom left). Biodiversity patterns on the different spatial topologies followed different trajectories between species-sorting and mass-effect regimes (see the leftmost panel and Fig. 1a). While the metacommunity with complete network (dashed line) reached the state of local coexistence (top left area) at the intermediate dispersal rate and shifted to a state of strong regional exclusion (bottom left), metacommunities with other topologies directly shifted to regional exclusion without exhibiting local coexistence. Moreover, the linear and tree topologies particularly retained relatively high gamma and beta diversity, i.e. they did not shift from species sorting to mass effects as much as other topologies at the highest dispersal rate.

theory. Specifically, we found that the nature of the transition between species-sorting and mass-effect regimes with increasing dispersal depends on both the pattern of dispersal connections across patches and autocorrelation in the environment. These two common features of real landscapes were not present in previous theoretical studies regarding the role of dispersal in controlling metacommunity dynamics.

Spatial topology dependence of the effect of dispersal process

While our results using the complete network (equivalent to a spatially implicit model) showed trends similar to the known hump-shaped relationship (i.e. high alpha diversity) (Mouquet and Loreau 2003), this relationship was not observed on other topologies. Moreover, by comparing biodiversity patterns calculated based on the Gini–Simpson index (Fig. 4) and species richness (Fig. 5), we showed that the hump-shaped relationship between alpha diversity and dispersal rate was more pronounced when measured with species richness as it is more sensitive to rare species than the Gini–Simpson diversity indices. The discrepancy in the diversity patterns observed between topologies implies that focusing on diversity patterns, particularly species richness, in a complete network gives an incomplete picture of metacommunity dynamics.

We also observed a trend that gamma diversity decreased as dispersal rate increased, indicating that regional competitive exclusion became stronger with higher dispersal rates. However, this effect was mediated by both the strength of local selection and the pattern of dispersal connections. When selection was strong, increasing dispersal did not strongly depress gamma diversity, and the complete network maintained the highest gamma diversity relative to other topologies through high levels of alpha diversity. This is because the source–sink effect became strong relative to regional competition on the complete network, which maintained high alpha diversity. When selection was weaker, increasing dispersal depressed gamma diversity through the regional competition of species, and this was strongest on the complete network relative to the other topologies (fourth rows in Fig. 4). In short, while the balance between source–sink effects and regional competition determines the biodiversity outcome, i.e. high local coexistence or regional exclusion, this balance was mediated by the strength of local selection and the pattern of dispersal connections.

While source–sink effects and local coexistence are often considered together as part of the mass-effect archetype with heterogeneous environment (Leibold et al. 2004), we have shown that the source–sink effect does not always support high local coexistence even when heterogeneous patches are connected by strong dispersal. Indeed, while high dispersal in the complete network effectively homogenized communities and reduced beta diversity to very low levels, beta diversity remained high in all the other networks even at high dispersal rates. In particular, gamma and beta diversity on the linear and tree networks were often much higher than other network topologies for a given level of total dispersal, and more tolerant to strong dispersal. This shows that mass effects were significantly weaker on the linear network relative to other networks due to the pattern of connections alone, and hence local selection became relatively stronger on these networks.

Our results showed that the consequence of increasing dispersal to high levels – high local coexistence (i.e. high alpha) or regional competitive exclusion (i.e. low gamma, beta, alpha) – depends on local selection strength, spatial network topology and spatial environmental autocorrelation. Local coexistence was enhanced the most in metacommunities with a completely connected topology, followed by grid and small-world, and linear or tree networks, depending on the level of spatial autocorrelation. This was reflected by beta diversity (gamma/alpha diversity), which is an indicator of heterogeneity in species composition across local communities.

The enhanced local coexistence on the complete network, coinciding with reduced regional exclusion, can be explained by the dense connections among patches. Local coexistence requires the dispersal of individuals of a particular species from their source patches to sink patches in sufficient numbers to offset negative growth rates within those sink patches. This means that patches with very dissimilar environments need to be adjacent to each other. Because individuals are exchanged between all pairs of patches on the complete network despite the extremely low dispersal rate on each connection, the mixing of species between their optimal and unfavourable patches happens regardless of the spatial arrangement of environmental conditions. By contrast, specific spatial arrangements of environmental conditions are required on other more sparse topologies for species to disperse to very dissimilar patches. Thus, such direct dispersal between very dissimilar patches is necessary for the source–sink effect to become more significant and to drive the mixing of local communities.

Emergence of environmental clusters at intermediate spatial scale

The linear and tree networks particularly enhanced local selection (Fig. 1a, 6). This enhancement was especially strong under weaker selection and higher spatial autocorrelation, as shown by their higher beta-diversity in species composition across local communities (third and fourth rows in Fig. 4). This can be explained by the formation of intermediate-scale dynamics as follows. Most nodes in the tree network and all nodes in the linear network are connected to few adjacent patches. Thus, on these networks it is more likely that adjacent patches have similar environmental conditions to each other than to other topologies, as long as spatial autocorrelation is positive (e.g. on the complete network, where all patches are connected to each other, it is impossible for a patch to be connected to only similar patches). Within clusters of patches with similar environmental conditions, community composition may be more easily homogenized and thus allow individuals to survive after dispersal. At the

same time, environmental boundaries between intermediate-scale clusters can separate them from each other and prevent homogenization between clusters, resulting in higher beta diversity.

The emergence of such environmental clusters is reflected by the different lower bounds in gamma diversity on different topologies as well (Fig. 6). Furthermore, there is a rise in beta and gamma diversity at high dispersal rates on linear network under the highest autocorrelation with $h = 0.1$ (leftmost panel in the second row in Fig. 4c). This rise is seemingly caused by strong dispersal between environmental clusters as boundaries are crossed, resulting in increased species sorting. Note that although network topologies and possible levels of spatial autocorrelation are tightly linked, there is a chance that such clusters can emerge within other network topologies in nature, especially when environmental heterogeneity among patches is limited. Also, the positive spatial autocorrelation often observed in nature and used in our simulations can on its own homogenize local communities between adjacent patches. However, what our results highlight is that for larger metacommunities and more heterogeneous environment, whether communities are homogenized at the regional scale is not trivial. Overall, we suggest that spatial structures in which most nodes have only a few connections likely enhance intermediate-scale dynamics. Such intermediate-scale dynamics can enhance the homogenization of community composition at the intermediate scale but prevent the homogenization at the regional scale, resulting in limiting regional exclusion.

Improved overview of the dispersal effect in species-sorting and mass-effect archetypes: linking spatial structure and biodiversity patterns

Overall, our results suggest that the balance between species sorting and mass effects depends both on the spatial topology and spatial autocorrelation. The complete network enhances mixing of individuals between patches, leading to higher local coexistence and a shift toward mass effects, whereas linear and tree networks tend to enhance local selection, resisting the transition to mass-effect dominated regime even at high dispersal. This is summarized in Fig. 1 and shown in Fig. 6. In the 2D-space of beta and gamma diversity, given the deterministic model dynamics assumed in the M&L model and the extended model used here, the right-top area corresponds to species sorting whereas the left area corresponds to mass effects. The transition from species sorting to mass effects can happen through a combination of source–sink effects and regional exclusion, as summarized in Fig. 1a. While dispersal rate is a main parameter that determines the balance between species sorting and mass effects under a given local selection strength, spatial topology and spatial autocorrelation are also involved in determining the trajectory of the transition. That is, whether the state of local coexistence (i.e. high alpha, high gamma and low beta) is realized, or both gamma and beta (thus alpha as well) monotonically decrease with increasing dispersal due to the dominant effect of regional exclusion with a lack of local coexistence. In other words, the prediction of the M&L model with its spatially implicit assumption seems to correspond to a particular case – when the mixing of communities between very dissimilar patches is significant relative to local selection strength. Such a situation is not always the case among a variety of spatial topologies. This trend – the higher local coexistence under the complete topology – seems analogous to the observation in a controlled experiment with fragmented moss-microarthropod systems in a heterogeneous environment by Chisholm et al. (2011), in which a continuous system in a heterogeneous environment supported higher alpha diversity than sparsely connected networks did. The mechanisms suggested here, that spatial topology and environmental autocorrelation affect biodiversity patterns particularly at the level of local coexistence, may explain this empirically observed patterns. However, this does not exclude the possibility that other dynamics such as interspecific interactions contributed to the patterns as well.

Our results link biodiversity patterns with different processes and conditions in a complex metacommunity. Among all the results shown in Fig. 4, gamma diversity was highest for the complete network under the strongest local selection. However, as local selection became weaker, gamma diversity became more dependent on total dispersal rate and environmental autocorrelation, and gamma diversity on linear and tree networks became higher than on other networks. In other words, when species are well adapted to the environment, densely-connected spatial structure maintains biodiversity the best through source–sink dynamics. By contrast, when species are less adapted to the environment, biodiversity becomes more sensitive to spatial processes and conditions (i.e. dispersal rate, dispersal trajectory and spatial arrangement of environments), and regional competition tends to exclude many suboptimal species, which corresponds to little local coexistence.

These complex relationships between metacommunity parameters may be a source of the controversy over the effect on biodiversity of corridors connecting fragmented patches (Haddad et al. 2014). Such a process-based understanding with detailed knowledge about ecosystems should provide the basis for improved conservation planning. For instance, our theoretical analysis indicates that when a system is more dominated by species sorting than mass effects, increasing connectivity (i.e. complete network) likely improves gamma diversity by increasing the chance of local coexistence (i.e. increasing alpha diversity). Moreover, it suggests that real landscapes may be able to avoid the negative effects of too much connectivity implied by mass effects – that regionally superior species swamp out other species that may be locally competitive. We found that the heterogeneous structure of dispersal and clusters of environmental similarity are able to resist mass effects by facilitating persistence of locally superior but globally inferior species in different regions of the network.

Our analysis is limited in a number of ways that suggest directions for future work. First, we focused on the transition between species-sorting and mass-effect archetypes, but

did not consider patch-dynamics and the neutral archetypes. Although the roles of spatially explicit structure have been explored within these archetypes to some extent (for example, for neutral theory in networks, Economo and Keitt 2008, Muneepeerakul et al. 2008), little is known about what governs the transitions between the archetypes. In the population genetics literature for example, different network structures have been known to amplify or depress the strength of drift versus selection (Lieberman et al. 2005). Thus, one could expect that landscape structure could mediate the balance between ecological drift and competition and whether neutral or deterministic competition dominates the dynamics. Likewise, the present analysis is based on adding a more complex spatial structure to the M&L model. Meanwhile, there are other assumptions of the model that could be relaxed, such as adding finite size effects, variation-in and evolution-of dispersal abilities, passive versus active dispersal and adding different carrying capacities across species.

Conclusion

Our results provide new insight into the species-sorting and mass-effect archetypes suggested by Leibold et al. (2004) and highlighted by the seminal studies of Mouquet and Loreau (2002, 2003). We analyzed the effect of complex metacommunity spatial structure on diversity patterns, and investigated how the balance between local and regional competitive dynamics are controlled by spatial structure. We found that as indicated by canonical results from Mouquet and Loreau (2003), increasing dispersal induced a transition from species sorting to mass effects across the metacommunity, as locally optimal species become increasingly replaced by regionally optimal species. However, the nature of that transition was highly dependent on the pattern of connections among local communities (network topology) and patterns of autocorrelation in the environment. Our results suggest the highly connected nature of a spatially implicit metacommunity results in dynamics that are not found in most spatially explicit structures. Notably, spatial structures with locally sparsely connected patches contribute to the emergence of intermediate-scale environmental clusters of patches. Such clusters can homogenize community composition at the intermediate scale. At the same time, the emergent boundaries between such clusters prevent homogenization at the regional scale, and this mechanism resulted in the reduction in mass effects. Understanding the effects of the spatial structure of dispersal and levels of environmental patchiness on biodiversity patterns provides a better theoretical understanding in community assembly, and has relevance for conservation problems.

Data availability statement

There are no empirical data used in this study. The code used to generate networks, simulate metacommunity dynamics and analyze results are included in the Supporting information. The networks used are also included.

Acknowledgements – We would like to thank Nicholas R. Friedman for thorough feedback and discussion. Both Y. S. and E. P. E. are supported by Okinawa Inst. of Science and Technology Graduate Univ. and its Scientific Computing and Data Analysis Section with the High Performance Computing.
Funding – Y. S. is additionally supported by JSPS KAKENHI Grant Number JP20J10699, and E. P. E. by JSPS Kakenhi Grant Number JP17K15180.

Author contributions

Yuka Suzuki: Conceptualization (equal); Formal analysis (lead); Funding acquisition (supporting); Investigation (lead); Methodology (lead); Project administration (supporting); Resources (lead); Validation (lead); Visualization (lead); Writing – original draft (lead); Writing – review and editing (equal). **Evan Economo**: Conceptualization (equal); Formal analysis (supporting); Funding acquisition (lead); Investigation (supporting); Methodology (supporting); Project administration (lead); Resources (supporting); Supervision (lead); Validation (supporting); Visualization (supporting); Writing – original draft (supporting); Writing – review and editing (equal).

References

Amarasekare, P. 2003. Competitive coexistence in spatially structured environments: a synthesis. – Ecol. Lett. 6: 1109–1122.
Amarasekare, P. and Nisbet, R. M. 2001. Spatial heterogeneity, source–sink dynamics and the local coexistence of competing species. – Am. Nat. 158: 572–584.
Bezanson, J. et al. 2017. Julia: a fresh approach to numerical computing. – SIAM Rev. 59: 65–98.
Cadotte, M. W. 2006. Dispersal and species diversity: a meta-analysis. – Am. Nat. 167: 913–924.
Chase, J. M. and Leibold, M. A. 2002. Spatial scale dictates the productivity–biodiversity relationship. – Nature 416: 427–430.
Chesson, P. 2000. Mechanisms of maintenance of species diversity. – Annu. Rev. Ecol. Syst. 31: 343–366.
Chesson, P. L. 1985. Coexistence of competitors in spatially and temporally varying environments: a look at the combined effects of different sorts of variability. – Theor. Popul. Biol. 28: 263–287.
Chisholm, C. et al. 2011. Metacommunity diversity depends on connectivity and patch arrangement in heterogeneous habitat networks. – Ecography 34: 415–424.
Cottenie, K. 2005. Integrating environmental and spatial processes in ecological community dynamics. – Ecol. Lett. 8: 1175–1182.
Crowley, P. H. 1981. Dispersal and the stability of predator–prey interactions. – Am. Nat. 118: 673–701.
Dias, P. C. 1996. Sources and sinks in population biology. – Trends Ecol. Evol. 11: 326–330.
Economo, E. P. and Keitt, T. H. 2008. Species diversity in neutral metacommunities: a network approach. – Ecol. Lett. 11: 52–62.
Gonzalez, A. et al. 2017. Spatial ecological networks: planning for sustainability in the long-term. – Curr. Opin. Environ. Sustain. 29: 187–197.

Haddad, N. M. et al. 2014. Potential negative ecological effects of corridors. – Conserv. Biol. 28: 1178–1187.
Hagberg, A. et al. 2008. Exploring network structure, dynamics and function using NetworkX. – Technical report, Los Alamos National Laboratory (LANL).
Harrison, S. and Cornell, H. 2008. Toward a better understanding of the regional causes of local community richness. – Ecol. Lett. 11: 969–979.
Heino, J. 2011. A macroecological perspective of diversity patterns in the freshwater realm. – Freshwater Biol. 56: 1703–1722.
Heino, J. et al. 2015. Metacommunity organisation, spatial extent and dispersal in aquatic systems: patterns, processes and prospects. – Freshwater Biol. 60: 845–869.
Hill, M. O. 1973. Diversity and evenness: a unifying notation and its consequences. – Ecology 54: 427–432.
Hillebrand, H. and Matthiessen, B. 2009. Biodiversity in a complex world: consolidation and progress in functional biodiversity research. – Ecol. Lett. 12: 1405–1419.
James, M. K. et al. 2002. The structure of reef fish metapopulations: modelling larval dispersal and retention patterns. – Proc. R. Soc. B 269: 2079–2086.
Jost, L. 2006. Entropy and diversity. – Oikos 113: 363–375.
Jost, L. 2007. Partitioning diversity into independent alpha and beta components. – Ecology 88: 2427–2439.
Jost, L. et al. 2010. Partitioning diversity for conservation analyses. – Divers. Distrib. 16: 65–76.
Kadmon, R. and Allouche, O. 2007. Integrating the effects of area, isolation and habitat heterogeneity on species diversity: a unification of island biogeography and niche theory. – Am. Nat. 170: 443–454.
Kininmonth, S. J. et al. 2010. Graph theoretic topology of the great but small barrier reef world. – Theor. Ecol. 3: 75–88.
Kneitel, J. M. and Chase, J. M. 2004. Trade-offs in community ecology: linking spatial scales and species coexistence. – Ecol. Lett. 7: 69–80.
Legendre, P. and Fortin, M. J. 1989. Spatial pattern and ecological analysis. – Vegetatio 80: 107–138.
Leibold, M. A. and Loeuille, N. 2015. Species sorting and patch dynamics in harlequin metacommunities affect the relative importance of environment and space. – Ecology 96: 3227–3233.
Leibold, M. A. and Norberg, J. 2004. Biodiversity in metacommunities: plankton as complex adaptive systems? – Limnol. Oceanogr. 49: 1278–1289.
Leibold, M. A. et al. 2004. The metacommunity concept: a framework for multi-scale community ecology. – Ecol. Lett. 7: 601–613.
Leibold, M. A. et al. 2017. Community assembly and the functioning of ecosystems: how metacommunity processes alter ecosystems attributes. – Ecology 98: 909–919.
Lieberman, E. et al. 2005. Evolutionary dynamics on graphs. – Nature 433: 312.
Loreau, M. et al. 2003. Biodiversity as spatial insurance in heterogeneous landscapes. – Proc. Natl Acad. Sci. USA 100: 12765–12770.
Morrissey, M. B. and de Kerckhove, D. T. 2009. The maintenance of genetic variation due to asymmetric gene flow in dendritic metapopulations. – Am. Nat. 174: 875–889.
Mouquet, N. and Loreau, M. 2002. Coexistence in metacommunities: the regional similarity hypothesis. – Am. Nat. 159: 420–426.
Mouquet, N. and Loreau, M. 2003. Community patterns in source–sink metacommunities. – Am. Nat. 162: 544–557.
Muko, S. and Iwasa, Y. 2000. Species coexistence by permanent spatial heterogeneity in a lottery model. – Theor. Popul. Biol. 57: 273–284.
Muneepeerakul, R. et al. 2007. A neutral metapopulation model of biodiversity in river networks. – J. Theor. Biol. 245: 351–363.
Muneepeerakul, R. et al. 2008. Neutral metacommunity models predict fish diversity patterns in Mississippi–Missouri basin. – Nature 453: 220–222.
Myers, J. A. and Harms, K. E. 2009. Seed arrival, ecological filters and plant species richness: a meta-analysis. – Ecol. Lett. 12: 1250–1260.
Petchey, O. L. et al. 1997. Effects on population persistence: the interaction between environmental noise colour, intraspecific competition and space. – Proc. R. Soc. B 264: 1841–1847.
Randin, C. F. et al. 2006. Are niche-based species distribution models transferable in space? – J. Biogeogr. 33: 1689–1703.
Shanafelt, D. W. et al. 2015. Biodiversity, productivity and the spatial insurance hypothesis revisited. – J. Theor. Biol. 380: 426–435.
Shanafelt, D. W. et al. 2018. Species dispersal and biodiversity in human-dominated metacommunities. – J. Theor. Biol. 457: 199–210.
Thompson, P. L. and Gonzalez, A. 2016. Ecosystem multifunctionality in metacommunities. – Ecology 97: 2867–2879.
Thompson, P. L. et al. 2017. Loss of habitat and connectivity erodes species diversity, ecosystem functioning and stability in metacommunity networks. – Ecography 40: 98–108.
Thompson, P. L. et al. 2020. A process-based metacommunity framework linking local and regional scale community ecology. – Ecol. Lett. 23: 1314–1329.
Tilman, D. 1994. Competition and biodiversity in spatially structured habitats. – Ecology 75: 2–16.
Vellend, M. 2016. The theory of ecological communities (MPB-57), Vol. 75. – Princeton Univ. Press.
Watts, D. J. and Strogatz, S. H. 1998. Collective dynamics of 'small-world' networks. – Nature 393: 440.
Wiens, J. A. 1989. Spatial scaling in ecology. – Funct. Ecol. 3: 385–397.
Witman, J. D. et al. 2004. The relationship between regional and local species diversity in marine benthic communities: a global perspective. – Proc. Natl Acad. Sci. USA 101: 15664–15669.